*Desalination and Water Treatment*
www.deswater.com
doi: 10.1080/19443994.2014.899928

54 (2015) 2324–2333
May

Taylor & Francis
Taylor & Francis Group

# Heterogeneous photodegradation of 1-naphthol with natural iron oxide in water: influence of oxalic acid

L. Mammeri*, T. Sehili, S. Belaidi, K. Djebbar

*Laboratory of Science and Technology of Environment, Faculty of Exact Sciences, Department of Chemistry, University of Constantine 1, Constantine 25000, Algeria, Tel. +213 31818867; email: l_mammeri@yahoo.fr*

Received 14 June 2013; Accepted 15 February 2014

ABSTRACT

The transformation of 1-Naphthol (1-NP) photoinduced by a natural iron oxide (NIO) in aqueous suspension and the influence of oxalic acid have been investigated under monochromatic irradiation (365 nm). The NIO was characterized by X-ray diffraction (XRD), X-ray fluorescence, and Brunauer–Emmett–Teller methods. The XRD result shows that the NIO consists of mixed crystalline hematite. A dark investigation of the system was performed before studying the photochemical behavior. The experiment shows that the NIO possesses a high adsorption capacity for 1-NP and its photodissolution was not observed. Also, the experiment shows that the UV light alone could play an important role in the degradation of 1-NP.After 3 h of irradiation at pH 9.4, 64.2% of 1-NP was degraded. The presence of the NIO was found to promote the photodegradation of 1-NP (72.1%) and the process follows pseudo-first-order reaction kinetics. The photodegradation of 1-NP has been studied at different pH (1.9–12) and catalyst loads (0.5–2.0 g $L^{-1}$). The results demonstrated that the phototransformation of 1-NP is enhanced by increasing the pH and the optimal initial concentration of the catalyst was found to be 1 g $L^{-1}$. The involvement of $^{\bullet}OH$ radicals was ruled out because of the non-influence of tertiobutanol used as a scavenger. The effect of the oxalic acid on the photodegradation of 1-NP by NIO was also investigated. The result revealed that the oxalic acid promoted the photodegradation rate of 1-NP. This investigation will give a new insight to understand the 1-NP photodegradation in natural environment. Measuring chemical oxygen demand also monitors the toxicity of the degraded 1-NP solution and a significant decrease is observed, which implies that the photodegradation through NIO is a safer technique.

*Keywords:* 1-Naphthol; Natural iron oxide; Oxalic acid; Heterogeneous photodegradation; Photodissolution

## 1. Introduction

Contamination of surface water and groundwater with aromatic compounds is one of the most serious environmental problems the world faces today [1]. Numerous treatment technologies to eliminate or reduce environmental problems have been developed, such as biodegradation, adsorption, and photocatalysis. The photocatalysis technology has been widely applied for degradation and mineralization of organic pollutants [2–4]. $TiO_2$ is the most commonly used material owing to its high photocatalytic activity,

*Corresponding author.

chemical stability, and non-toxicity. However, because of its wide band-gap energy (3.2 eV), $TiO_2$ can only absorb wavelengths in the near ultraviolet (UV) region ($\lambda < 400$ nm), which significantly hinders its practical application [5,6]. Consequently, while using the solar energy, the photocatalyst should acquire small band-gap energy less than 3 eV casing the major part of solar spectrum. In this regard, iron oxide, which acquires small band-gap energy of 2.3 eV, is one of the best materials to utilize solar energy efficiently [7]. Adsorption is another widely used environmental treatment technology. Adsorption techniques have potential for removing organics from water due to their high efficiency and ability to separate a wide range of chemical compounds [8,9].

Iron oxides have been widely used as adsorbents in wastewater treatment to remove organic and inorganic pollutants [10–17]. Iron oxides, on the other hand, are good alternatives for pollutants' degradation under visible light because of their stability, non-toxicity, simple production, low cost, and abundance in nature. In fact, there have been several success reports using $Fe_2O_3$ and FeOOH as photocatalysts for degradation of various pollutants such as chlorophenols [18], aminophenols [19–21], 2,6-dimethylphenol [22], atrazine [23], phenol [24,25], salicylic acid [26], and dyes [27–29], although their efficiencies are quite low.

In fact, iron oxides and oxalic acid, which coexist together in aquatic environments, can form a photochemical system to conduct a photo-Fenton-like reaction with much higher quantum efficiency than that of the $Fe(OH)^{2+}$ photochemical process or the photocatalytic reaction with iron oxides alone [30–35]. Oxalic acid is first adsorbed on the surface of iron oxide to form iron oxide–oxalate complexes of $[\equiv FeIII(C_2O_4)_n]^{3-2n}$, which can be excited to form a series of radicals including oxalate radical $(C_2O_4)^{\bullet-}$, carbon-centered radical $(CO_2)^{\bullet-}$, superoxide ion $(O_2^{\bullet-})$, $^{\bullet}OOH$, and hydroxyl radical ($^{\bullet}OH$). This hydroxyl radical attacks the organic pollutants and is effective in their mineralization.

1-Naphthol (1-NP), a large-scale hazardous industrial chemical used for the manufacture of dyes, insecticides, etc., is a metabolite of the insecticide carbaryl (1-naphthyl methylcarbamate). Also, it affects the reproductive hormone levels in adult men [36]. 1-NP, which is one of the major by-products of naphthalene degradation, is discharged from many industries, such as dye, plastics, synthetic rubber, and asbestos production, and is known to have similar toxicity to naphthalene [37]. In addition, due to the substituted hydroxyl group, it has a much higher solubility in water than naphthalene, which can result in high levels of contamination in aquatic and soil environments through enhanced mobility. Because 1-NP can be released in the environment, it is of great interest to investigate the processes of 1-NP degradation that can occur in the aquatic environment. The natural iron oxide (NIO) used in this work comes from a mineral in Chaabet-El-Ballout, which is located in Souk-Ahras, northeast of Algeria. The analysis of the iron deposits from Chaabet-El-Ballout revealed that they are mostly composed of hematite $Fe_2O_3$.

In this paper, we present the results of our investigation on the photodegradation kinetics of 1-NP in aqueous NIO suspensions. Several key factors such as the amount of the photocatalyst, initial 1-NP concentration, oxygen, and pH value were studied to determine the optimum treatment conditions. A dark investigation of the system NIO-water-1-NP was performed before studying the photochemical behavior. The role of oxalic acid in this photochemical process was also demonstrated.

## 2. Experimental

### 2.1. Materials

The NIO was washed several times with distilled water and dried at 45°C. 1-NP (99% + Acros Organics), sodium hydroxide (NaOH, 98% Carlo Erba Reagenti), hydrochloric acid (HCl, 37% Merck), acetate sodium (99%), acetic acid (99.5%), and sulfuric acid (98%) were provided by Panreac. 1,10 phenantroline (>99% Fluka), titanium (IV) oxysulfate solution (Sigma Aldrich, Fluka analytical), oxalic acid (99.5% Prolabo), dichromate (Aldrich), and methanol (99% VWR Prolabo) were used without further purification. Deionized water (18.2 mΩ cm) from an ultrapure water system (Simplicity UV, MILLIPORE) was used in all experiments.

### 2.2. Characterization

The chemical composition of NIO fractions was obtained by X-ray Fluorescence (CUBIX, PANALYTICAL Ex PHILIPS). The crystalline phase formed in the sample was determined by X-ray powder diffraction (XRD, D8 Advance Bruker NXS) with monochromated Cu-Kα radiation (40KV, 40 mA). The specific surface area ($S_{BET}$) and total pore volume of NIO sample were determined by the multipoint BET method using $N_2$ as the adsorbate (Quantachrome instruments, USA).

### 2.3. Experimental setup and procedure

Degradation experiments were performed in containers made up of stainless steel cylinders, built upon

a circular base. The solution was irradiated in a Pyrex glass tube. It was placed vertically in the center of the cylinder and irradiated by medium pressure mercury lamps (Philips HPW 125) emitted at 365 nm. The photoreactor tubes were placed in a Pyrex glass jacket of a slightly larger diameter flushed by water; thus providing cooling and keeping constant temperature of the irradiated solution. The solutions were magnetically stirred during irradiations.

The reactor was first filled with the suspension containing hematite particles. The required volume of 1-NP solution (50 mL) or mixed solution of 1-NP and oxalic acid was then added. The mixture was rapidly fed. When necessary, the solutions were deoxygenated at room temperature by continuous nitrogen bubbling in the reactor. The samples withdrawn at different reaction times were filtered with cellulose acetate filters (0.45 μm) to separate NIO particles. All experiments were performed at $T = 293 \pm 1$ K. The solution pH was adjusted by 1.0 M of HCl or NaOH and measured by means of an HANNA Instruments 8521 pH meter. Chemical oxygen demand (COD) digestion apparatus (Thermoreaktor CR 3200) was used for determining COD.

### 2.4. Analytical methods

The remaining 1-NP during the photodegradation was determined by HPLC (Shimadzu) equipped with a controller model SCL-10A VP, photodiode-array UV–vis detector model SPD-M10A VP, and two pumps model LC 8A. The system is controlled by software "Class VP5" for storing and processing of chromatograms. The analytical column is a C18 Supelco (5 μm, 250 × 4.6 mm i.d). The methanol–ultrapure water mixture (55:45) was used at mobile flow rate of 1 mL $min^{-1}$ at room temperature. The detection wavelength was at 290 nm. The UV–vis absorption spectra were recorded employing a Unicam «Hελios α» spectrophotometer controlled by software "Vision". Fe (II) concentration was determined by the method of Zuo [38] with o-phenantroline by measuring the absorbance at 510 nm of the complex (the molar absorption coefficient: 11,040 $M^{-1}$ L $cm^{-1}$ [39]). Hydrogen peroxide was determined using titanium (IV) oxysulfate according to DIN 38402H15.

## 3. Results and discussion

### 3.1. Catalyst properties

The NIO was analyzed by X-ray Fluorescence. The chemical composition of NIO fractions is summarized in Table 1. The X-ray diffraction (XRD) pattern as shown in Fig. 1 confirmed that the NIO sample has nine characteristic peaks of (012), (104), (110), (113), (024), (116), (018), (214), and (300) attributable to hematite [40] and three additional peaks at $2\theta = 21.2$, 29.5, and 36.67°. The specific surface area of hematite was 79.02 $m^2/g$ and the total pore volume was 0.0893 $cm^3/g$. The results show that the NIO is not pure and contains predominantly hematite $Fe_2O_3$.

### 3.2. Characterization of 1-NP

The UV–visible spectra of 1-NP ($10^{-4}$ M) in aqueous solution at experimental pH (pH 6.5) pointed out in Fig. 2 shows a maximum absorption at $\lambda = 290$ nm ($\varepsilon = 4{,}560 \pm 200$ L $M^{-1}$ $cm^{-1}$) and a shoulder around 320 nm. For pH values above the pKa 1-NP (pKa = 9.3), the shape of the UV–Visible spectrum substrate changes because the anionic form is predominant. The absorption spectrum of the anionic form as shown in Fig. 2 has two strips at 245 nm and the other at 332 nm. There was a band shift of 42 nm. We can note the good recovery of UV absorption spectrum substrate and the solar emission spectrum. Thus, it may undergo a phototransformation in the aquatic environment.

### 3.3. Behavior of 1-NP-NIO system in absence of irradiation

A dark investigation of the system 1-NP-NIO was performed before studying the photochemical behavior. The solution containing mixture of 1-NP-NIO ($10^{-4}$ M, 1 g $L^{-1}$) kept in dark at 20°C was not stable in terms of loss of 1-NP, when the mixture ages (Fig. 3). Disappearance of 1-NP due to the addition of NIO observed might be related to adsorption of 1-NP to NIO under our experimental conditions.

The kinetics of 1-NP disappearance obtained by HPLC and spectrophotometric (Fig. 3) indicate similar

Table 1
Chemical composition of NIO fractions obtained by X-ray fluorescence

| Compound formula | Composition (%) |
|---|---|
| $SiO_2$ | 4.75 |
| $Al_2O_3$ | 0.38 |
| $Fe_2O_3$ | 76.06 |
| CaO | 2.64 |
| MgO | 0.17 |
| Cl | 0.008 |
| $Na_2O$ | 0.000 |
| $K_2O$ | 0.026 |
| $SO_3$ | 0.04 |

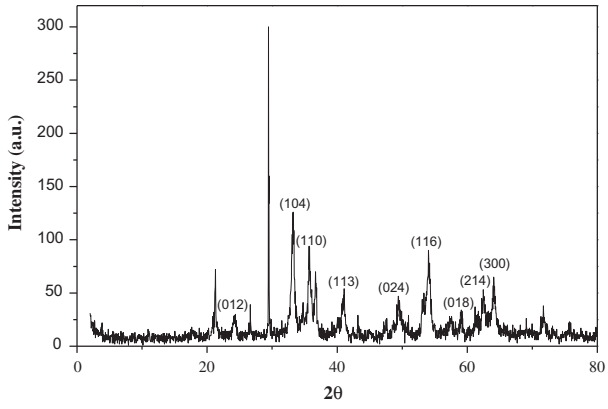


Fig. 1. XRD pattern of the NIO.

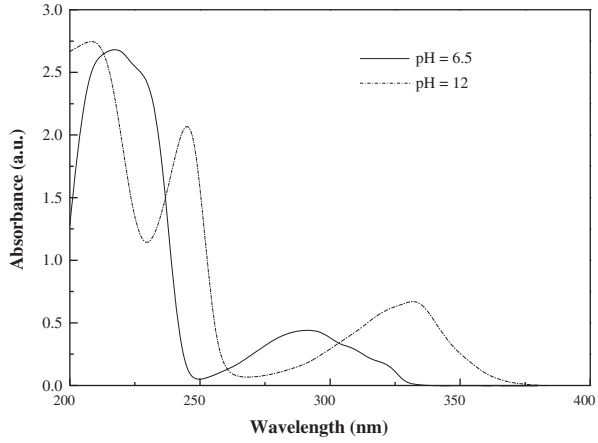


Fig. 2. UV–Visible spectrum of 1-NP ($10^{-4}$ M) in aqueous solution.

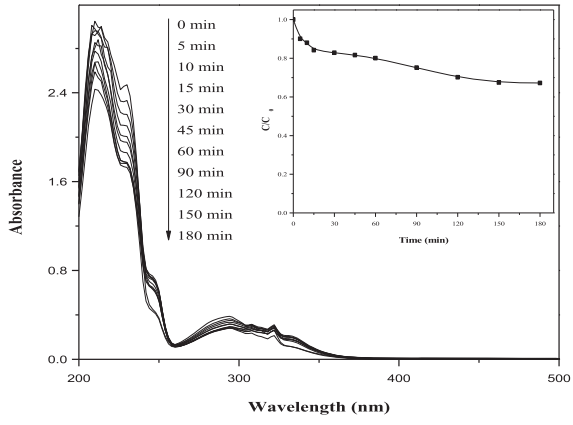


Fig. 3. UV–Visible spectral changes of 1-NP ($10^{-4}$ M) in the mixture 1-NP/NIO ($10^{-4}$ M, 1 g $L^{-1}$) in the dark at 20°C and at natural pH = 9.4. The insert shows the absorbance changes of 1-NP at 292 nm.

behavior showing a slight decrease which becomes more important when the solution ages.

The chromatograms obtained during this reaction do not show any formation of intermediate product. These results confirm an adsorption on the surface of NIO. The adsorption rate of 1-NP on the surface of NIO particles obtained after 3 h of experimental examination was 30.96%.

### 3.3.1. Fe(II) formation

The presence of Fe(II) resulting from the dissolution of $Fe_2O_3$ was checked out in the filtered aliquots by complexometry with ortho-phenantroline. Under our experimental conditions, we were unable to detect any release of iron II in the suspension either in the presence or in the absence of 1-NP.

### 3.3.2. Effect of pH

The mixture of 1-NP-NIO ($10^{-4}$ M, 1 g $L^{-1}$) at pH 2, 9.4, and 12 were followed at different times. The kinetics of disappearance of 1-NP at natural and acidic pH follows similar pattern as shown in Fig. 4. However, at the basic pH, the rate of disappearance of 1-NP is 1.5% after 3 h.

The point of zero charge of hematite is $pH_{pzc}$ = 8.5–9.48 [40]. At pH's < ppzc, the $FeOH_2^+$ groups predominate over $FeO^-$ groups, i.e. the surface has a net positive charge. The adsorption of the catalyst on 1-NP is the result of the formation of a monodentate surface complex, due to a chelation of electron donator group (–OH) with the active site of $Fe_2O_3$ (Fig. 5). The $pK_a$ of 1-NP is equal to 9.3, for pH values higher than $pK_a$; the adsorption of 1-NP in basic media is deprived by the repulsive forces which exist between the anionic form of the substrate, predominant in this pH range, and the surface negatively charged of $Fe_2O_3$ ($FeO^-$). This explains the decrease in the amounts adsorbed.

The percentages of the 1-NP disappearance deduced from the kinetics at different pH (Table 2) show that the efficiency of adsorption is higher in acidic medium.

### 3.4. Photochemical behavior of 1-NP-NIO system

The irradiation experiments were carried out immediately after mixing the reactants. This permits us to neglect the contribution of the thermal processes since the time scale of these processes is much larger than the time scale of the irradiation processes.

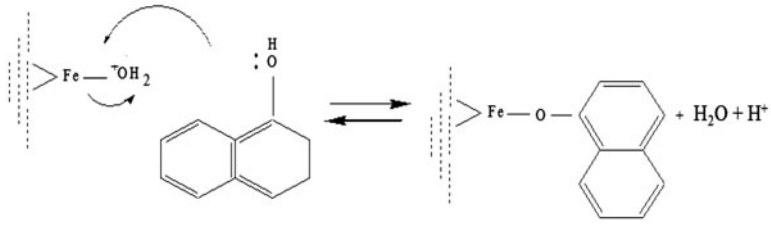


Fig. 4. Pathway of 1-NP adsorption on the surface of $Fe_2O_3$.

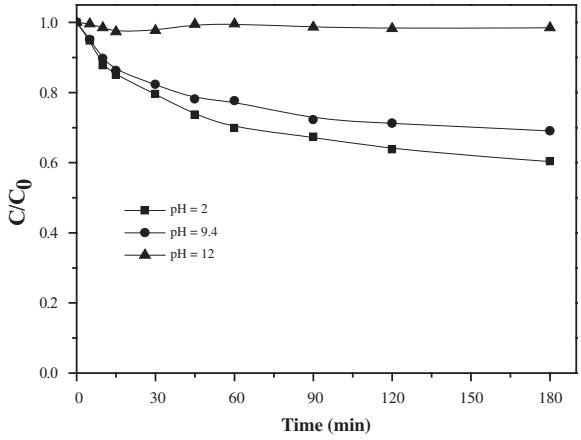


Fig. 5. Disappearance of 1-NP during thermal reaction in the mixture 1-NP-NIO ($10^{-4}$ M, 1 g $L^{-1}$) at different pH levels.

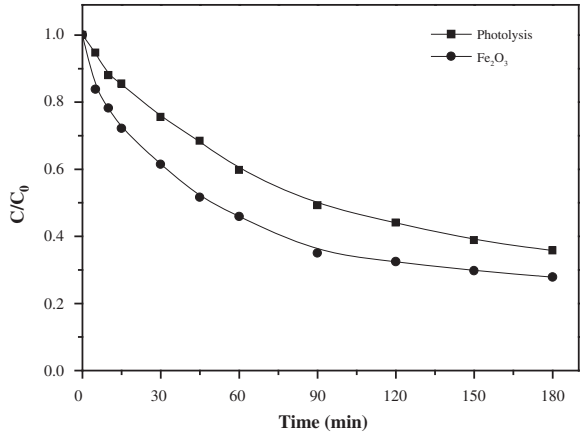


Fig. 6. Disappearance of 1-NP ($10^{-4}$ M) in absence and in the presence of $Fe_2O_3$ (1 g.$L^{-1}$) under irradiation at 365 nm and at pH = 9.4.

Table 2
Percentages of disappearance of 1-NP in the mixture 1-NP-NIO ($10^{-4}$ M, 1 g $L^{-1}$) at different pH levels

| pH | Disappearance rate (%) |
|---|---|
| 2 | 39.70 |
| 9.4 | 30.96 |
| 12 | 1.50 |

### 3.4.1. Photodegradation of 1-NP by NIO

The elimination of 1-NP was studied at two different experimental conditions: under UV illumination in absence of NIO (photolysis) and under UV illumination in presence of NIO (photocatalysis). In Fig. 6, the concentration of 1-NP is plotted as a function of reaction time. It can be observed that 1-NP could be transformed by UV light alone ($\lambda = 365$ nm).After 3 h of illumination at pH 9.4, 64.2% of 1-NP was degraded. However, in the presence of the NIO, the photodegradation of 1-NP was promoted.

Iron (II) produced by charge separation in the photoredox reaction was followed by complexometry. The result showed that there no iron (II) was detected under our conditions.

### 3.4.2. Influence of catalyst loading

Fig. 7 showed the effect of the $Fe_2O_3$ dosages on the photodegradation of 1-NP with the initial concentration of $10^{-4}$ M. The pH almost remained constant during the course of the experiment, suggesting that $Fe_2O_3$ has buffer capacity due to the charged surface groups ($\equiv FeOH_2^+$, $\equiv FeOH$, $\equiv FeO^-$) [41].

An electron hole pair ($h_{vb}^+/e_{cb}^-$) is formed when a photon with energy greater than the band gap of α-$Fe_2O_3$, which is an active photocatalyst, is adsorbed. The hole valence band ($h_{vb}^+$) [$E_H = 2.3$ eV] is a powerful oxidant and the electron conduction band ($e_{cb}^-$) [$E_H = 0.0$ eV] is a relatively poor reductant. The catalytic power of α-$Fe_2O_3$ is generally less effective compared to $TiO_2$, because of the fast recombination of ($h_{vb}^+/e_{cb}^-$). This can be due to a high density of intrinsic mid-band gap electronic states, internal defect induced trap states, and, to a lesser extent, surface defects [42,43].

The first-order kinetic constants $k$ were $6.69 \times 10^{-3}$ ($R^2 = 0.9459$), $12.16 \times 10^{-3}$ ($R^2 = 0.9825$), $8.26 \times 10^{-3}$ ($R^2 = 0.9363$), and $8.01 \times 10^{-3}$ ($R^2 = 0.9868$) $min^{-1}$ with the dosage of 0.5, 1.0, 1.5, and 2.0 g $L^{-1}$ of $Fe_2O_3$, respectively. Obviously, there should be an optimal dosage

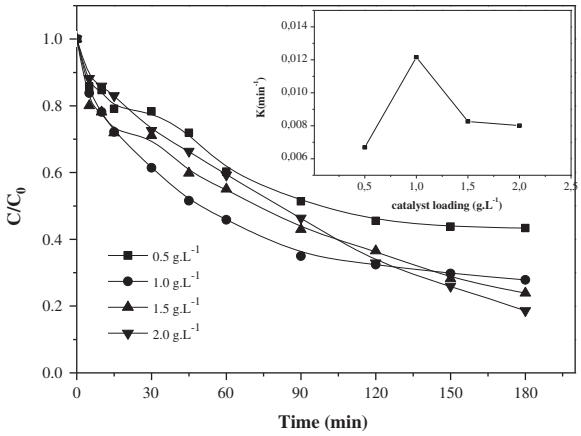


Fig. 7. The effect of NIO dosage on the photodegradation of 1-NP ($10^{-4}$ M) under UV irradiation at pH = 9.4.

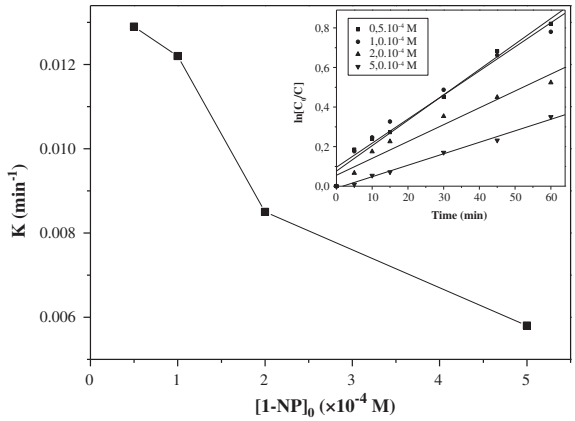


Fig. 8. Plots of In $[C_0/C]$ vs. irradiation time for 1-NP photodegradation runs carried out in the presence of $Fe_2O_3$ (1 g $L^{-1}$) and various concentrations of 1-NP.

of 1 g $L^{-1}$ for $Fe_2O_3$. In fact, excessive dosage of iron oxide will limit the penetration of UV light in the solution and lead to the quick decay of UV light intensity.

### 3.4.3. Influence of 1-NP concentration

Experiments were carried out under different 1-NP initial concentrations in the 1-NP- $Fe_2O_3$ system at the natural pH of 9.4.

1-NP photodegradation by $Fe_2O_3$ was found to occur according to the Langmuir–Hinshelwood rate law, i.e.:

$$r = -\frac{dC}{dt} = \frac{kKC_0}{1 + KC_0} \quad (1)$$

The equation can be simplified to a pseudo-first-order equation:

$$\ln\frac{C_0}{C} = kKt = \mathrm{k't} \quad (2)$$

The lines on the top right corner of the graph in Fig. 8 were derived by plotting ln $[C_0/C]$ vs. time. The first-order rate constants $k'$ (Table 3), represent the slope of these plots. The experimental results obtained (Table 3) show that the apparent kinetic constant $k'$ decreased with increasing 1-NP concentration. In other words, the apparent kinetic constant $k'$ is inversely proportional to $C_0$ ($C_0$ is the initial 1-NP concentration). Therefore, it can be derived that the photodegradation of 1-NP by $Fe_2O_3$ follows a pseudo-first-order kinetics.

### 3.4.4. Influence of pH

The effect of the pH on the rate of photodegradation of 1-NP was examined in the range 1.9–12 in an aqueous NIO suspension. The results are depicted in Fig. 9. The enhancing effect of increasing pH was due to a higher oxidability of the anionic form of 1-NP in comparison with the molecular form.

### 3.4.5. Influence of oxygen

1-NP-NIO suspensions ($10^{-4}$ M, 1 g $L^{-1}$) were irradiated at 365 nm in deoxygenated (nitrogen bubbling), aerated, and oxygen-saturated system. The corresponding kinetics of disappearance of 1-NP represented in Fig. 10 illustrate that oxygen seems to be necessary for 1-NP degradation.

### 3.4.6. Influence of tertiobutanol on the 1-NP-NIO system

Tertiobutanol 1% (v/v) was added to some 1-NP-NIO suspensions in order to give evidence for the formation of $^{\bullet}OH$ radicals. Actually, tertiobutanol is commonly used to quench hydroxyl radicals, the

Table 3
Photodegradation kinetics data of 1-NP by $Fe_2O_3$

| $C_0$ (M) | $k'$ ($min^{-1}$) | $R^2$ |
|---|---|---|
| $0.5 \times 10^{-4}$ | 0.0129 | 0.9893 |
| $1 \times 10^{-4}$ | 0.0122 | 0.9825 |
| $2 \times 10^{-4}$ | 0.0085 | 0.9759 |
| $5 \times 10^{-4}$ | 0.0058 | 0.9959 |

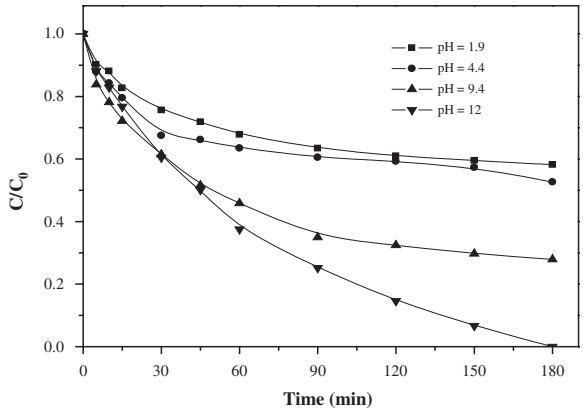


Fig. 9. Effect of pH on the photodegradation rate of 1-NP in presence of 1 g $L^{-1}$ $Fe_2O_3$, $[1\text{-NP}]_0 = 10^{-4}$ M.

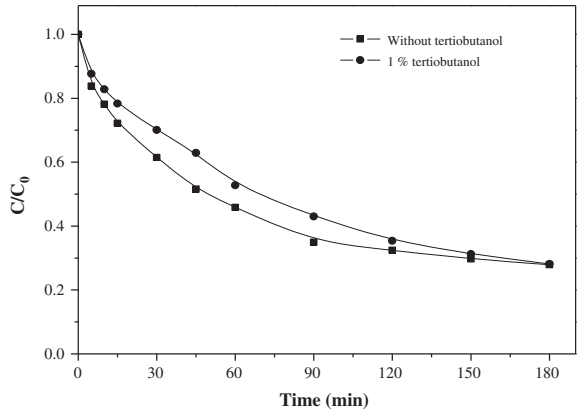


Fig. 11. Kinetics of 1-NP disappearance upon irradiation of 1-NP/$Fe_2O_3$ ($10^{-4}$ M-1 g $L^{-1}$) at 365 nm in the presence and in absence of tertiobutanol.

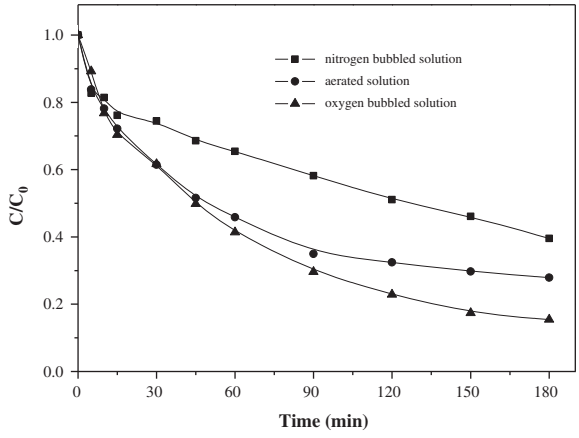


Fig. 10. Photodegradation of deoxygenated, aerated, and oxygen saturated 1-NP-$Fe_2O_3$ slurries at pH = 9.4. $[Fe_2O_3]_0$ = 1 g $L^{-1}$, $[1\text{-NP}]_0 = 10^{-4}$ M.

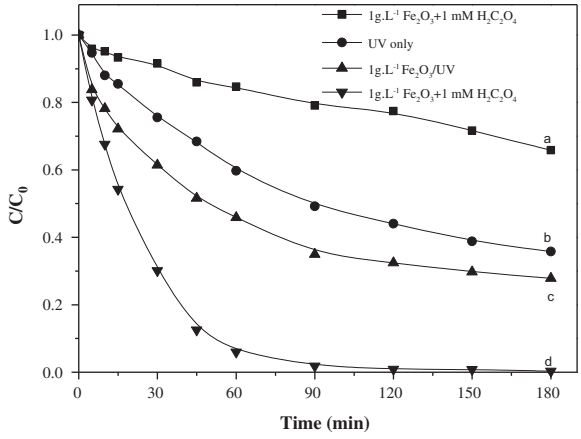


Fig. 12. Photodegradation of 1-NP ($10^{-4}$ M) in different systems 1 g $L^{-1}$ NIO, 1 mM oxalic acid.

rate constant of the reaction between $^{\bullet}OH$ and tertiobutanol is $6 \times 10^8$ $M^{-1}$ $s^{-1}$ [44]. It was observed that the degradation of 1-NP was not affected by the presence of the alcohol (Fig. 11). It can be deduced that hydroxyl radicals are not involved in the process of 1-NP degradation.

### 3.5. Influence of oxalic acid

Fig. 12 shows the degradation of 1-NP with an initial concentration ($C_{1\text{-NP}}$) $10^{-4}$ M under different reaction conditions. Without UV light (dark) and only with 1 mM oxalic acid and 1 g $L^{-1}$ NIO, 1-NP concentration was decreased by 34.1% because 1-NP was adsorbed on the surface of the NIO (curve a). Under UV illumination without iron oxide and oxalic acid, the removal percentage of 1-NP was about 64.2% after 3 h (curve b). Under UV illumination with 1 g $L^{-1}$ NIO and without oxalic acid, the removal percentage of 1-NP was 72.1% after 3 h and its first-order kinetic constant was determined to be $0.45 \times 10^{-2}$ $min^{-1}$ (curve c). When both 1 mM oxalic acid and 1 g $L^{-1}$ NIO were added into the 1-NP solution under UV illumination (curves d), the removal percentage of 1-NP was significantly increased up to 99.7% after 3 h reaction and its first-order kinetic constant was determined to be $4.5 \times 10^{-2}$ $min^{-1}$. The results indicate that the combination of iron oxide, oxalate, and UV light is essential for 1-NP's photodegradation. The photochemical process in the presence of iron oxide and oxalate together has been described in detail [45–47]. During the photochemical reaction of Fe(III)−oxalate complexes, many key intermediates are formed through the

reactions, shown in Eqs. (3)−(8). These intermediates include dissolved Fe(II) and Fe(III) species, adsorbed Fe(II) and Fe(III) species, and the superoxides and hydroperoxyl radicals ($O_2^{\bullet-}/{}^{\bullet}OOH$). $H_2O_2$ can be obtained by the dismutation of $O_2^{\bullet-}/{}^{\bullet}OOH$, as per Eqs. (9) and (10). After $H_2O_2$ was formed, the classical Fenton reaction takes place with Fe(II) species (the photo-reduction products of Fe(III) species) to form ${}^{\bullet}OH$, as Eq. (11). This was the reason why 1-NP photodegradation was enhanced greatly in the presence of oxalate.

$$\text{Iron oxide} + n\ H_2C_2O_4 \leftrightarrow [\equiv Fe(C_2O_4)_n]^{(2n-3)-} \quad (3)$$

$$[\equiv Fe(C_2O_4)_n]^{(2n-3)-} + h\nu \rightarrow Fe(C_2O_4)_2^{2-} \ (\text{or } \equiv Fe(C_2O_4)_2^{2-}) + (C_2O_4)^{\bullet-} \quad (4)$$

$$Fe^{III}(C_2O_4)_n^{3-2n} + h\nu \rightarrow [Fe^{II}(C_2O_4)_{(n-1)}]^{(4-2n)} + (C_2O_4)^{\bullet-} \quad (5)$$

$$(C_2O_4)^{\bullet-} \rightarrow CO_2 + CO_2^{\bullet-} \quad (6)$$

$$CO_2{}^{\bullet-} + O_2 \rightarrow CO_2 + O_2^{\bullet-} \quad (7)$$

$$O_2{}^{\bullet-} + H^+ \rightarrow {}^{\bullet}OOH \quad (8)$$

$$O_2{}^{\bullet-} + Fe^{3+} \rightarrow Fe^{2+} + O_2 \quad (9)$$

$$O_2^{\bullet-}/{}^{\bullet}OOH + nH^+ + Fe^{2+} \rightarrow Fe^{3+} + H_2O_2 \quad (10)$$

$$Fe^{2+} + H_2O_2 \rightarrow Fe^{3+} + OH^- + {}^{\bullet}OH \quad (11)$$

### 3.5.1. The formation of $Fe^{2+}$and hydrogen peroxide

It can be seen from Fig. 12 that the photodecomposition of 1-NP is faster with the NIO and the oxalic acid than that with NIO alone because in the absence of oxalic acid, no dissolved $Fe^{2+}$ was found and no $H_2O_2$ was detected within 3 h of irradiation (data not shown). On the other hand, in the presence of oxalic acid, small amounts of dissolved $Fe^{2+}$ in the range of 0.01–0.18 mM were detected, as illustrated in Fig. 13. Dissolved $Fe^{2+}$ will react with $H_2O_2$ generated (Eq. 10) to form the most reactive oxidant (${}^{\bullet}OH$) in this system. In the dark, dissolved $Fe^{3+}$ was formed by the desorption of surface Fe(III)-oxalate complexes, and Fe(II) was generated by the slow reductive dissolution.

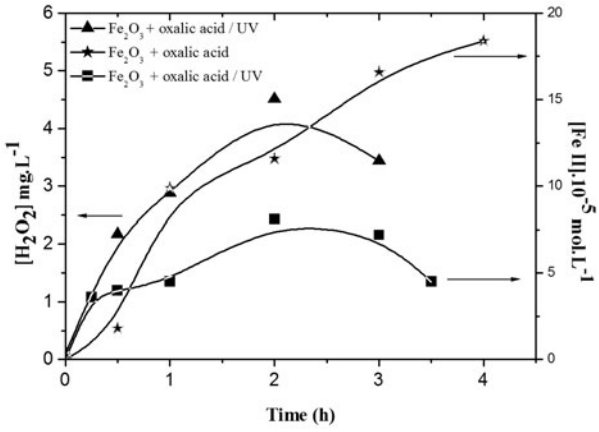


Fig. 13. The variation of dissolved $Fe^{2+}$ and $H_2O_2$ during 1-NP photodegradation under an initial concentration of 1 mM oxalic acid.

### 3.5.2. Influence of tertiobutanol on the 1-NP-NIO-oxalic acid system

Contrary to the disapperance of 1-NP in the mixture 1-NP/NIO, that was insensitive to tertiobutanol, the degradation of 1-NP in the mixture 1-NP/NIO/Oxalic acid ($10^{-4}$ M, 1 g $L^{-1}$, 1 mM) was 26.1% inhibited in the presence of 1% of tertiobutanol (Fig. 14). Thus, the transformation is not only due to hydroxyl radicals. Another reactive species, which does not react with alcohol, is necessarily involved. This species are most probably positive holes $h^+$ formed on the irradiated photocatalyst, which react with the adsorbed molecules.

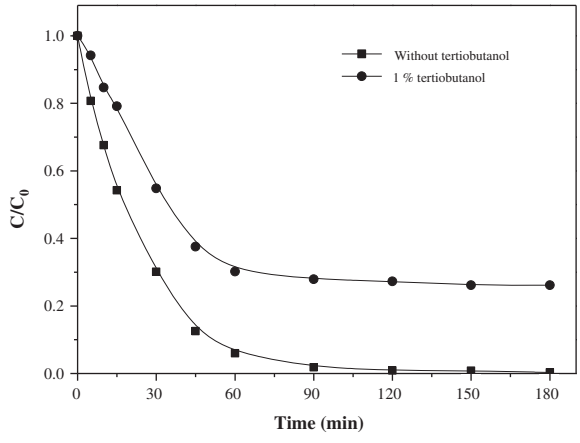


Fig. 14. Effect of tertiobutanol on the photodegradation of 1-NP ($10^{-4}$ M) in presence of NIO (1 g $L^{-1}$) and oxalic acid (1 mM).

## 4. Chemical oxygen demand

The COD is an effective technique to measure the strength of organic content present in wastewater. This test allows the measurement of total quantity of oxygen required for the complete oxidation of organic matter to carbon dioxide and water. In order to verify that the 1-NP encountered a total mineralization, the COD of its solution was determined before and after the treatment. This was performed on the two processes studied in this paper (with NIO alone and with NIO/Oxalate systems). To measure the COD, we used the method presented by Thomas and Mazas [48]. We observed a significant decrease in the COD values of the1-NP solution from 36.80 to 3.31 mg $L^{-1}$ in the case of the photocatalyzed process with NIO and from 99.84 to 3.04 mg $L^{-1}$ in the case of photocatalyzed process with NIO/Oxalate. The significant decrease in the COD values indicates the high potential of the NIO-catalyzed photodegradation processes for the removal of 1-NP from wastewater.

## 5. Conclusion

The experiments confirmed the efficiency of the NIO used in this study for the degradation of 1-NP. The photodegradation of 1-NP depended significantly on various factors including the initial pH value, the amount of iron oxide and the presence of oxygen. A reduction of the consumption rate of 1-NP has been recorded decreasing the pH of the solution. An important effect of oxygen was observed. The results indicate that the oxidation process is not sustained by the intervention of $^{\bullet}OH$ radicals as for other photocatalytic systems and the formation of iron (II) could not be detected in 1-NP-NIO-UV system. The existence of oxalic acid together with NIO can achieve much faster degradation of 1-NP in aqueous solution than NIO alone.

## References

[1] W. Zhang, J. Chen, B. Pan, Q. Zhang, Cooperative adsorption behaviours of 1-naphthol and 1-naphthylamine onto nonpolar macroreticular adsorbents, React. Funct. Polym. 66 (2006) 485–493.
[2] V.K. Gupta, R. Jain, A. Mittal, T.A. Saleh, A. Nayak, S. Agarwal, S. Sikarwar, Photo-catalytic degradation of toxic dye amaranth on $TiO_2$/UV in aqueous suspensions, Mater. Sci. Eng., C 32 (2012) 12–17.
[3] R. Jain, M. Mathur, S. Sikarwar, A. Mittal, Removal of the hazardous dye rhodamine B through photocatalytic and adsorption treatments, J. Environ. Manage. 85 (2007) 956–964.
[4] V.K. Gupta, R. Jain, A. Mittal, M. Mathur, S. Sikarwar, Photochemical degradation of the hazardous dye Safranin-T using $TiO_2$ catalyst, J. Colloid Interface Sci. 309 (2007) 464–469.
[5] M. Addamo, V. Augugliaro, A. Di Paola, E. García-López, V. Loddo, G. Marcì, R. Molinari, L. Palmisano, M. Schiavello, Preparation, characterization, and photoactivity of polycrystalline nanostructured $TiO_2$ catalysts, J. Phys. Chem. B 108 (2004) 3303–3310.
[6] J.C. Yu, L. Zhang, Z. Zheng, J. Zhao, Synthesis and characterization of phosphated mesoporous titanium dioxide with high photocatalytic activity, Chem. Mater. 15 (2003) 2280–2286.
[7] S.U.M. Khan, J. Akikusa, Photoelectrochemical splitting of water at nanocrystalline n-$Fe_2O_3$ thin-film electrodes, J. Phys. Chem. B 103 (1999) 7184–7189.
[8] D.B. McGregor, A.G. Brown, S. Howgate, D. McBride, C. Riach, W.J. Caspary, Responses of the L5178Y mouse lymphoma cell forward mutation assay. V: 27 coded chemicals, Environ. Mol. Mutagen. 17 (1991) 196–219.
[9] F.L. Slejko, Adsorption Technology: A Step-by-Step Approach to Process Evaluation and Application, Marcel Dekker, New York, NY, 1985.
[10] J. Bandara, J. Mielczarski, J. Kiwi, 1. Molecular mechanism of surface recognition. Azo dyes degradation on Fe, Ti, and Al oxides through metal sulfonate complexes, Langmuir 15 (1999) 7670–7679.
[11] C.R. Evanko, D.A. Dzombak, Surface complexation modeling of organic acid sorption to goethite, J. Colloid Interface Sci. 214 (1999) 189–206.
[12] J. Hur, M.A. Schlautman, Molecular weight fractionation of humic substances by adsorption onto minerals, J. Colloid Interface Sci. 264 (2003) 313–321.
[13] Z. Pan, P. Somasundaran, N.J. Turro, S. Jockusch, Interactions of cationic dendrimers with hematite mineral, Colloids Surf., A 238 (2004) 123–126.
[14] M.R. Das, D. Bordoloi, P.C. Borthakur, S. Mahiuddin, Kinetics and adsorption of benzoate and salicylate at the natural hematite–water interface, Colloids Surf., A 254 (2005) 49–55.
[15] B.H. Jeon, B.A. Dempsey, W.D. Burgos, R.A. Royer, E.E. Roden, Modeling the sorption kinetics of divalent metal ions to hematite, Water Res. 38 (2004) 2499–2504.
[16] N. Xu, C. Christodoulatos, W. Braida, Modeling the competitive effect of phosphate, sulfate, silicate, and tungstate anions on the adsorption of molybdate onto goethite, Chemosphere 64 (2006) 1325–1333.
[17] Y.S. Hwang, J.J. Lenhart, Surface complexation modeling of dual-mode adsorption of organic acids: Phthalic acid adsorption onto hematite, J. Colloid Interface Sci. 336 (2009) 200–207.
[18] J. Bandara, J.A. Mielczarski, A. Lopez, J. Kiwi, 2. Sensitized degradation of chlorophenols on iron oxides induced by visible light: Comparison with titanium oxide, Appl. Catal., B 34 (2001) 321–333.
[19] C. Pulgarin, J. Kiwi, Iron oxide-mediated degradation, photodegradation, and biodegradation of aminophenols, Langmuir 11 (1995) 519–526.
[20] J. Bandara, K. Tennakone, J. Kiwi, Surface mechanism of molecular recognition between aminophenols and iron oxide surfaces, Langmuir 17 (2001) 3964–3969.
[21] R. Andreozzi, V. Caprio, R. Marotta, Iron(III) (hydr) oxide-mediated photooxidation of 2-aminophenol in aqueous solution: A kinetic study, Water Res. 37 (2003) 3682–3688.

[22] P. Mazellier, M. Bolte, Heterogeneous light-induced transformation of 2,6-dimethylphenol in aqueous suspensions containing goethite, J. Photochem. Photobiol., A 132 (2000) 129–135.
[23] E. Pelizzetti, C. Minero, V. Carlin, photoinduced degradation of atrazine over different metal oxides, New J. Chem. 17 (1993) 315–319.
[24] S. Chatterjee, S. Sarkar, S.N. Bhattacharyya, Photodegradation of phenol by visible light in the presence of colloidal $Fe_2O_3$, J. Photochem. Photobiol., A 81 (1994) 199–203.
[25] B. Pal, M. Sharon, Preparation of iron oxide thin film by metal organic deposition from Fe(III)-acetylacetonate: A study of photocatalytic properties, Thin Solid Films 379 (2000) 83–88.
[26] B. Pal, M. Sharon, Photocatalytic degradation of salicylic acid by colloidal $Fe_2O_3$ particles, J. Chem. Technol. Biotechnol. 73 (1998) 269–273.
[27] J. Bandara, J. Mielczarski, J. Kiwi, 2. Photosensitized degradation of azo dyes on Fe, Ti, and Al oxides, mechanism of charge transfer during the degradation, Langmuir 15 (1999) 7680–7687.
[28] W. Du, Y. Xu, Y. Wang, Photoinduced degradation of orange II on different iron (Hydr)oxides in aqueous suspension: Rate enhancement on addition of hydrogen peroxide, silver nitrate, and sodium fluoride, Langmuir 24 (2008) 175–181.
[29] W. Du, Q. Sun, X. Lv, Y. Xu, Enhanced activity of iron oxide dispersed on bentonite for the catalytic degradation of organic dye under visible light, Catal. Commun. 10 (2009) 1854–1858.
[30] C. Siffert, B. Sulzberger, Light-induced dissolution of hematite in the presence of oxalate: A case study, Langmuir 7 (1991) 1627–1634.
[31] B.C. Faust, R.G. Zepp, Photochemistry of aqueous iron(III)-polycarboxylate complexes: Roles in the chemistry of atmospheric and surface waters, Environ. Sci. Technol. 27 (1993) 2517–2522.
[32] Y. Zuo, Y. Deng, Iron(II)-catalyzed photochemical decomposition of oxalic acid and generation of $H_2O_2$ in atmospheric liquid phases, Chemosphere 35 (1997) 2051–2058.
[33] F. Gulshan, S. Yanagida, Y. Kameshima, T. Isobe, A. Nakajima, K. Okada, Various factors affecting photodecomposition of methylene blue by iron-oxides in an oxalate solution, Water Res. 44 (2010) 2876–2884.
[34] Q. Lan, H. Liu, F.b. Li, F. Zeng, C.S. Liu, Effect of pH on pentachlorophenol degradation in irradiated iron/oxalate systems, Chem. Eng. J. 168 (2011) 1209–1216.
[35] S. Belaidi, T. Sehili, L. Mammeri, K. Djebbar, Photodegradation kinetics of 2,6-dimetylphenol by natural iron oxide and oxalate in aqueous solution, J. Photochem. Photobiol., A 237 (2012) 31–37.
[36] J.D. Meeker, L. Ryan, D.B. Barr, R. Hauser, Exposure to nonpersistent insecticides and male reproductive hormones, Epidemiology 17 (2006) 61–68.
[37] S.J. Stohs, S. Ohia, D. Bagchi, Naphthalene toxicity and antioxidant nutrients, Toxicology 180 (2002) 97–105.
[38] Y. Zuo, Kinetics of photochemical/chemical cycling of iron coupled with organic substances in cloud and fog droplets, Geochim. Cosmochim. Acta 59 (1995) 3123–3130.
[39] E. Rodríguez, M. Mimbrero, F.J. Masa, F.J. Beltrán, Homogeneous iron-catalyzed photochemical degradation of muconic acid in water, Water Res. 41 (2007) 1325–1333.
[40] R.M. Cornell, U. Schwertmann, The Iron Oxides: Structure, Properties, Reaction, Occurrences and Uses, 2nd ed., Wiley–VCH, Weinheim, 2003.
[41] H. Fu, X. Quan, H. Zhao, Photodegradation of γ-HCH by α-$Fe_2O_3$ and the influence of fulvic acid, J. Photochem. Photobiol., A 173 (2005) 143–149.
[42] R.D. Stramel, J.K. Thomas, Photochemistry of iron oxide colloids, J. Colloid Interface Sci. 110 (1986) 121–129.
[43] N.J. Cherepy, D.B. Liston, J.A. Lovejoy, H. Deng, J.Z. Zhang, Ultrafast studies of photoexcited electron dynamics in γ- and α-$Fe_2O_3$ semiconductor nanoparticles, J. Phys. Chem. B 102 (1998) 770–776.
[44] G.V. Buxton, C.L. Greenstock, W.P. Helman, A.B. Ross, Critical review of rate constants for reactions of hydrated electrons, hydrogen atoms and hydroxyl radicals ($^{\bullet}OH$ /$O^{\bullet-}$) in aqueous solution, J. Phys. Chem. Ref. Data 17 (1988) 513–886.
[45] M.E. Balmer, B. Sulzberger, Atrazine degradation in irradiated iron/oxalate systems: effects of pH and oxalate, Environ. Sci. Technol. 33 (1999) 2418–2424.
[46] P. Mazellier, B. Sulzberger, Diuron degradation in irradiated, heterogeneous iron/oxalate systems: The rate-determining step, Environ. Sci. Technol. 35 (2001) 3314–3320.
[47] X. Wang, C. Liu, X. Li, F. Li, S. Zhou, Photodegradation of 2-mercaptobenzothiazole in the γ-$Fe_2O_3$/oxalate suspension under UVA light irradiation, J. Hazard. Mater. 153 (2008) 426–433.
[48] O. Thomas, N. Mazas, Chemical oxygen demand measurement in a not very polluted environment, Analusis 14 (1986) 300–302.